Available online at www.sciencedirect.com

ScienceDirect

Energy Procedia 81 (2015) 732 – 741

Energy Procedia

69th Conference of the Italian Thermal Engineering Association, ATI 2014

Numerical Evaluation of the Applicability of Steady Test Bench Swirl Ratios to Diesel Engine Dynamic Conditions

Forte Claudio[a], Catellani Cristian[a], Cazzoli Giulio[a,*], Bianchi Gian Marco[a], Falfari Stefania[a], Brusiani Federico[a], Verzè Alessandro[b], Saracino Stefano[b]

[a]*Department of Industrial Engineering, University of Bologna, V.le del Risorgimento 2, Bologna 40122, Italy*
[b]*VM Motori S.p.a., Via Ferrarese 29, Cento (FE) 44042, Italy*

Abstract

Engine coherent flow structures such as swirl and tumble motions are key factors for the combustion process due to their capability to rise turbulence levels and enhance mixing which, in turns, severely influence both fuel efficiency and pollutant emissions. Automotive industry has therefore put great efforts over the last decades in evaluating air flow during induction stroke and air flow within the cylinder. Nowadays swirl and tumble motion characterizing a specific cylinder head are evaluated experimentally at design stage mainly using stationary flow benches. Such tests allow characterizing each head prototype using non-dimensional parameters like swirl and tumble ratios and, finally, to compare the different designs. In the present work the authors focused their attention on the swirl ratio characterization, firstly reviewing the two main methodologies for evaluating such parameter and more precisely the AVL and the Ricardo ones. A numerical method is then proposed in order to reproduce the stationary test bench with the final goal to develop a fast and accurate virtual test bench for cylinder head design. Simulations have been carried out on different VM Motori engine heads for which experimental data were available. The comparison between computational and experimental swirl ratios allowed to evaluate the suitability of using a virtual test bench as alternative or complementary to experiments. These results widened the understanding of the swirl fluid-dynamics and suggested that care must be taken when comparing duct designs having no geometrical similarity. Finally dynamic simulations have been performed for the head prototypes in order to compute the engine swirl in realistic conditions and to compare it with the steady bench results. This allowed evaluating the capability of the two different "static" swirl ratio definition (AVL/Ricardo) in correctly estimating real engine swirl.

Peer-review under responsibility of the Scientific Committee of ATI 2014

Keywords: Flow bench; Diesel engine; Swirl Ratio; CFD

* Corresponding author. Tel.: +39-0512093316; fax: +39-0512093316.
E-mail address:giulio.cazzoli@unibo.it

Peer-review under responsibility of the Scientific Committee of ATI 2014
doi:10.1016/j.egypro.2015.12.079

1. Introduction

The increasing severity of legislation on vehicles pollutant emissions and fuel consumption like the forthcoming EURO VI [1] strongly demands for a better design of internal combustion engines. Automotive industry is therefore putting great effort in order to improve vehicle performances acting on factors such as aerodynamics, weight reduction, tribology and engine efficiency.

Among others, combustion efficiency is one of the key factors determining engine performance [2]. For this reason, engine coherent flow structures such as swirl and tumble motions are subject of severe study and optimization for each new engine at design stage. These coherent flow motions play in fact a key role in the combustion process due to their capability to rise turbulence levels and enhance mixing between fuel and air influencing both fuel efficiency and pollutant emissions [3,4,5,6,7]. Car makers R&D has a strong interest in evaluating air motion during induction stroke and air flow within the cylinder. In particular, swirl and tumble motion characterization of a specific cylinder head is performed experimentally mainly using stationary flow benches [8]. These tests allow characterizing each head prototype using non-dimensional parameters like Swirl and Tumble Ratios [9,10] and, finally, to compare the different designs. Unfortunately no standardized testing methodology exists at present and great care has to be taken when comparing data coming from different sources. A comprehensive review of the most widely adopted techniques can be found in [11].

Direct measurement of swirl in dynamic engine operation is currently feasible only with test engines equipped with optical access, by using LDV or PIV techniques [11]. Other methods include the “water analogue” test rig [12,13] and the Imperial Collage pulse flow arrangement [14]. The expensiveness of the aforementioned methodologies has driven researchers towards the development of alternative techniques employing cheaper and faster stationary testing.

In the present work the authors focused their attention on the swirl ratio characterization with a twofold objective: firstly, numerical steady simulation is considered evaluating its potential as a substitute to experimental stationary bench tests, then, the link between steady and dynamic swirl ratio is assessed in order to verify the capability of steady testing to effectively describe the dynamic engine head performance.

2. Steady flow testing methodology

Swirl motion is usually evaluated through a non-dimensional parameter called Swirl Ratio R_s which is the ratio between two characteristic angular velocities defined as:

$$R_S = \frac{\omega_d}{\omega_m} \tag{1}$$

where ω_d is an average rotational velocity of the charge free vortex and ω_m is an engine reference rotational velocity. The quantity ω_d is evaluated considering the charge vortex as a rigid body rotating about its own axis, so that its angular momentum can be calculated by summation of the angular momentum contributions at each crank angle (CA) all over the intake stroke.

2.1. Swirl Number definitions

While the Swirl Ratio characterizes the swirl providing integral information about the engine head performance all over the intake stroke, another quantity, the Swirl Number provides useful information about the swirl strength at a specific time during intake i.e. for a specific valve lift. Swirl Number N_s is evaluated in a similar manner to the R_s, that is by taking the ratio between a characteristic engine charge velocity and an engine reference velocity. The Swirl Ratio will be therefore calculated as a weighted average of the Swirl Numbers characterizing an engine head with different weights varying upon the formulation. Two popular choices are the following:

- the Rig Swirl Number (proposed by Ricardo):

$$N_{SR} = \frac{\omega_s R}{V_0} \tag{2}$$

- the Stationary Swirl Number (proposed by AVL):

$$N_{SA} = \frac{\omega_s}{\omega_m} \tag{3}$$

Ricardo called its parameter “Rig Swirl Number” defining it as the ratio between the average tangential velocity of the free vortex and the incompressible ideal velocity V_0 trough the duct:

$$V_0 = \sqrt{\frac{2\Delta_p}{\rho}} \tag{4}$$

where Δ_p is the pressure drop across the duct, ρ is the density and R is the cylinder radius. AVL named its parameter “Stationary Swirl Number” and defines it as the ratio between the vortex angular velocity and the engine rotational speed. To be noted that $\omega_d \neq \omega_s$. While ω_d represents a an engine parameter at θ_{IVC}, ω_s represents a flow bench parameter, evaluated for a specific valve lift.

After some mathematical passages, here not reported for sake of brevity but available in [15], the two expressions can be reformulated as:

$$N_{SR} = \frac{8}{\dot{m} B V_0} M \tag{5}$$

$$N_{SA} = \frac{2S}{\rho \dot{Q}^2} M \tag{6}$$

where B is the cylinder bore, $\dot{m}$ is the mass flow rate, $\dot{Q}$ is the volumetric flow rate, S is the stroke length and M is the torque-meter measure accordingly to the technique of choice (Ricardo or AVL) as described in [16] or [17]. Given the two definitions here proposed, the corresponding AVL and Ricardo Swirl Ratio will present different formulations.

2.2. Flow Coefficient evaluation

If the Swirl Number is a fundamental quantity needed to evaluate the Swirl Ratio, the Flow Coefficient is another important parameter as well. It represents the ratio between the measured mass flow rate through the valve port and the theoretical mass flow rate through a reference area of the port/valve system and provides information on the permeability of the engine head:

$$C_E = \frac{\dot{m}}{\rho A_{ref} V_0} \tag{7}$$

where A_{ref} is a specific reference area of choice. The most widely employed ones are the following:

- valve seat area
- minimum section area (critical section)
- valve external diameter area
- curtain area, dependent on the valve lift

In the present work the first definition has been adopted so that

$$A_{ref} = \frac{\pi D_V^2}{4} \tag{8}$$

with D_V being the valve seat diameter.

2.3. Swirl ratio evaluation

The angular momentum conservation equation can be expressed as:

$$\frac{dL}{dt} = M \tag{9}$$

where L is the angular momentum. With regards to the general definition of Swirl Ratio, (9) can be rearranged as:

$$L = \frac{1}{4} R^4 \omega \rho 2\pi S = \int_{t_{IVO}}^{t_{IVC}} M \, dt \tag{10}$$

Introducing in (10) the definitions of Flow Coefficient and Swirl Number it is possible to obtain:

$$R_{SR} = \frac{\omega_d}{\omega_m} = \frac{BS}{n_V D_V^2} \frac{\int_{\theta_{IVO}}^{\theta_{IVC}} C_E N_{SR} \, d\theta}{\left(\int_{\theta_{IVO}}^{\theta_{IVC}} C_E \, d\theta \right)^2} \tag{11}$$

$$R_{SA} = \frac{1}{\pi} \int_0^{\pi} N_{SA} \left[\frac{v(\theta)}{v_m} \right]^2 d\theta \tag{12}$$

where (11) and (12) are the Swirl Ratio definitions accordingly to Ricardo and AVL respectively. The main difference between the two lies in the range of integration: Ricardo considers the full intake stroke between IVO and IVC while AVL considers the angular interval between TDC and BDC only. Furthermore it is clear from (12) how AVL managed to link its definition to a non-dimensional piston velocity thanks to the term in square brackets, in which $v(\theta)$ is the instantaneous piston velocity (depending on the CA) and v_m is the mean piston velocity. Such term weights the contribution of the N_{SA} respect to the piston motion, which, in turns, is the event promoting the intake flow.

The relation between the two definition can be expressed as:

$$\frac{N_{SR}}{N_{SA}} = \frac{n_v \pi D_V^2 C_E}{BS} \tag{13}$$

where n_v is the number of intake valves. As it can be seen, the relationship between N_{SR} and N_{SA} is not trivial and it depends on C_E varying with valve lift.

Fig. 1: Engine head type A

Fig. 2: Engine head type B

Fig. 3: Engine head type C

Fig. 4: Engine head type D

3. Simulation methodology

In figures 1-4 are reported the geometries object of the present study. For each head-duct assembly CAD models and experimental data have been provided by VM Motori. The tested prototypes are the following:

- A 2 valves heavy duty Diesel engine (Fig. 1)
- B 4 valves heavy duty Diesel engine (Fig. 2)
- C 4 valves automotive Diesel engine (Fig. 3)
- D 4 valves automotive Diesel engine (Fig. 4)

3.1. Current practice for steady bench testing

In industry the most widely adopted instruments for swirl measurement are the paddle wheel [17] and the flow torque-meter [16]. Several works have proved the former method not to be particularly reliable in the measure due to its interaction and disturbance of the flow and the friction of the wheel bearings. The torque-meter has therefore become the instrument of choice in recent years. It must be noted that the position of the torque-meter influences the measurement of swirl: Ricardo recommends to place it 1.75 times the cylinder bore distant from the head firing surface as a compromise between allowing the vortex to develop and limiting its decay. Other authors suggest to perform the measurement even farther away from the head (about 3 times the cylinder bore) to allow swirl stabilization and to permit the flow center to better align the cylinder axis. However, in the current work, the $1.75B$ distance rule has been adopted since the experimental data provided by VM Motori has been obtained using such setup.

3.2. Numerical model for steady flow bench

In order to create a virtual test bench, a specific CFD methodology has been developed. All the analyses have been carried out using the CFD code AVL Fire 2010. The computational domain is reported in figures 5 and 6 and it comprises the intake ducts, the engine head, the intake valves and the cylinder liner. For each valve lift a different geometry has been used. Hexa-dominant meshes have been generated taking care of the near-wall flow resolution for which four wall layers have been employed. The discretized domains so obtained counted nearly two millions elements each.

VM Motori carried out the experimental campaign on the head prototypes employing an impulse torque meter, accordingly to Ricardo methodology. Such instrument, from a fluid-dynamic perspective acts damping out tangential velocity components causing at the same time a pressure drop across itself.

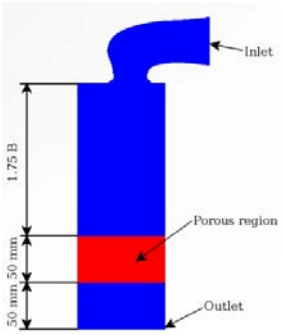

Fig. 5: Computational domain for the virtual steady flow bench and porous domain location

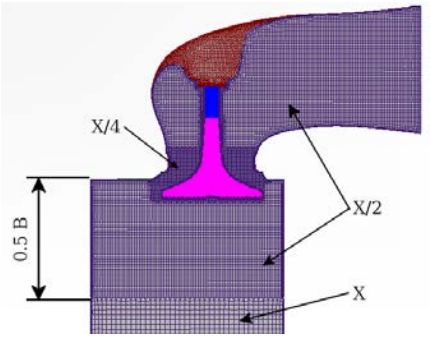

Fig. 6: Grid refinement levels

In order to reproduce the presence of the impulse torque-meter a porous medium has been introduced inside the cylinder. The porous medium has been modeled using the Darcy-Forchaimmer model available in AVL Fire 2010 [18]:

$$\frac{dp}{dx} = -\alpha \mu u - \beta \frac{\rho}{2} u^2 \tag{14}$$

where x is the cylinder axis direction, u is the velocity component along such direction and the porosity parameters α and β have been determined experimentally by VM Motori and kindly made available to the authors.

Accordingly to Ricardo testing methodology [16] the impulse swirl meter has to be placed at a distance of 1.75*B* from the head. Therefore the porous region reproducing it begins at 1.75*B* from the head extending for 50 mm inside the cylinder. Finally other 50 mm are left past the porous medium to stabilize outflow conditions as it can be seen in figure 5.

The mesh base size is 2 mm and as visible in figure 6 several discretization refinements have been applied to the computational grid in order to properly resolve the flow features. In particular one eighth of the base mesh size has been used close to the walls and one fourth for the valve throat region.

A fixed static pressure has been set at both inlet and outlet sections and the values for each tested engine head are reported in table 1. The pressure difference applied to the system is close to the value suggested by Ricardo and equals to 500 mmH_2O.

The fluid used was air at ambient conditions modeled as ideal gas (see table 1 for inflow conditions). AVL Fire 2010 pressure-based compressible solver has been adopted along with a blended first/second order advection scheme as optimal compromise between accuracy and robustness. A high-Re *k-ζ-f* model has been chosen for turbulence modeling and wall functions have been used to treat fluid flow at solid surfaces.

Table 1: Boundary conditions employed for the steady state analyses

Parameter Name	Units	Value
Inlet Static Pressure	[mbar]	1012
Overall Pressure Drop	[mmH2O]	500
Inlet Temperature	[°C]	25

Post-processing of results dealt primarily with the evaluation of mass flow rate and torque. Both quantities have been evaluated runtime though a cut plane perpendicular to cylinder axis and located 1 mm upstream the porous region to avoid possible disturbances in the sampling. Since some cases showed a mass flow rate slightly oscillating about a mean value, the average over the last 2000 iterations have been taken. The torque has been evaluated through a user function accordingly to equation (10) and subsequent derivations available in [15].

3.3. Dynamic analyses methodology

The dynamic analyses have been carried out modifying the grids in order to reproduce the engines operating conditions by adding pistons and motion capabilities. In particular the piston bowl shape strongly influences the swirl development inside the cylinder, so that this feature represents one of the key differences between static and dynamic testing. Fluid properties are the same as for the steady simulations. Intake valve lift profile, engine speed and boundary conditions have been provided by VM Motori. For all the prototypes only the intake stroke has been simulated and the Swirl Number has been sampled at each timestep.

4. Results

4.1. Steady Flow Bench

The results obtained for the stationary flow bench simulations are synthesized in table 3 where they are compared to the experimental averages. Comparisons between numerical and experimental results are shown in figures 7-10 As it can be seen, the computed Swirl Ratios are in good agreement with the measurements. The most significant discrepancy is found for prototype B: figures 9 and 10 make evident the peculiar behavior of this engine respect to the other models.

In particular, the Swirl Number of engine B drops at a lift of about $h / D_s = 0.15$. Furthermore it can be seen how, at medium/high valve lifts, where the Swirl Number are lowest, the weighting functions, i.e. the C_E are the highest, thus amplifying the reduction in the computed Swirl Ratio. Moreover, looking at engine B N_{SR} trend, this presents an inflection point for the aforementioned h / D_s lift value, after which the N_{SR} tends to diminish with lift. None of the other prototypes presents such feature, not even engine A, which is the closest in tendency to engine B. It must also be noted that this peculiar behavior holds for the experimental data as shown in figure 10.

In order to establish the causes of the different performance of engine B respect to the other prototypes, the CFD 3D fields have been analyzed in detail. It has then been found that at $h / D_s = 0.15$ flow detachment occurs for both intake ducts. Figure 11 show the fully developed detachment. This happens when the flow limiting area switches from the valve curtain area to the valve seat area. However since other engine models present the same detachment phenomenon without significant drops in the Swirl Ratio, the cause of engine B behavior has to be found elsewhere. It is in the authors' opinion that a possible explanation can be inferred looking at the engine geometrical parameters, the most significant ones reported in table 2. It is evident, in fact, how the valve/seat diameter ratio for engine B appears to be out of scale/off-scale respect to the other prototypes. Such deviation from the geometrical similitude is even magnified if considering the valve/seat area or the valve/cylinder area ratios.

Table 2 permits to make some considerations about AVL and Ricardo Swirl Ratio: results basically demonstrate an equal capability of the two formulations in properly approximating the experimental ratios and thus both can be considered equally eligible for virtual testing application

Table 2: Characteristic geometric parameters for the tested engines

Prototype	A	B	C	D
Stroke/Bore	1.14	1.11	1.06	1.11
n_v	1	2	2	2
$\phi_{valve} / \phi_{seat}$	1.14	1.28	1.15	1.13
Stroke/(2 Conrod)	0.33	0.32	0.31	0.28

The results obtained for steady state analyses allow to say that the computational methodology here proposed is a reliable substitute of experiments for engine heads comparison as long as the prototypes dimensional parameters satisfy geometric similitude. When such requirement is not satisfied the virtual testing presents some limitations in its capability to accurately predict fluid-dynamic behavior of prototypes, as seen for engine B. Further and deeper investigations are needed in order to assess the cause of the phenomenon and this will be the object of future work.

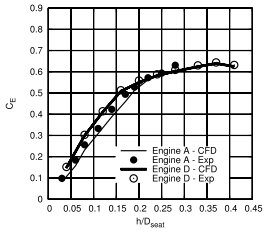

Fig.7: Numerical and experimental C_E for engines A and D

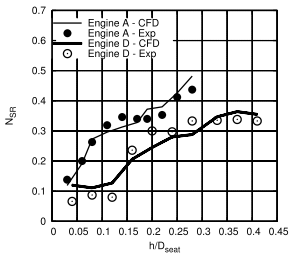

Fig.8: Numerical and experimental N_{SR} for engines A and D

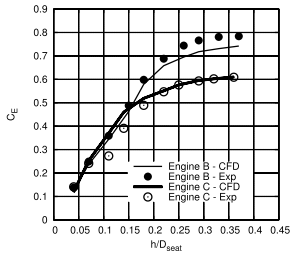

Fig. 9: Numerical and experimental C_E for engines B and C

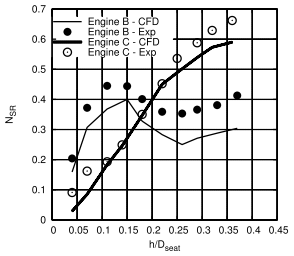

Fig. 10:Numerical and experimental N_{SR} for engines B and C

4.2. Dynamic Testing

The correlation between static and dynamic results can be done considering the duct operating in unsteady conditions as a sequence of steady states for both permeability and flow development, i.e. by considering the process as quasi-static. Previous static testing has shown the capabilities of CFD in emulating a flow bench. This ensures that an eventual disagreement between static and dynamic results is not a limitation of the CFD methodology or of the code in use, but it's rather due to the difficulty of properly establishing a link between stationary and dynamic operating conditions. The formulas proposed represent therefore the tentative of overcoming such limitations. Unfortunately the dynamic simulation has a number of features that the static one is intrinsically missing which severely influence flow development into the cylinder and, worstly, which is impossible to evaluate in a steady flow bench. The most important of such features is the piston bowl shape moving accordingly to crank-slider function and whose shape strongly influences the flow field whereas, in the stationary bench, the flow is free to develop up to the torque-meter. Furthermore it must be noted that the valve motion isn't a 1 mm step ramp, but it is a smooth bell-shaped curve, presenting therefore the same lift twice within the angular interval between θ_{IVO} and θ_{IVC}, one in the opening ramp and one in the closing ramp. Table 3 summarizes the results obtained for experiments and computations. Dynamic testing results appear not to be always aligned to stationary ones. More precisely the agreement appears satisfactory for engine D only, making it hard to establish a direct correlation between stationary and dynamic testing Swirl Ratios.

The comparison for steady and dynamic results for a selected case (engine C) are reported in figure 12 where noticeable differences appear. As it can be seen both magnitude and shape of mass flow rate and torque differ. The most significant difference is the lack of symmetry of the dynamic simulation. For the same valve lift the results differ between opening and closing phases, this suggesting a dependency of the swirl development and thus the Swirl Number from the valve dynamics. Furthermore, for both mass flow rate and torque the peaks aren't properly resolved with the most significant discrepancy found for the former quantity. It is in the authors' belief that improvements can be obtained in the R_S estimation by adopting an alternative approach.

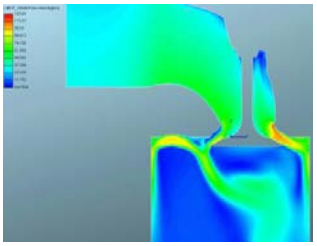

Fig. 11: Engine B - Detached flow for $h / D_s = 0.22$

Table 3: Comparison between experimental and computational Swirl Ratios

Prototype	Experimental R_S		CFD R_S		CFD R_S
	Ricardo	AVL	Ricardo	AVL	Dynamic
A	1.75	2.31	1.92	2.53	1.56
B	1.47	1.89	1.21	1.54	1.74
C	1.51	2.11	1.55	2.20	1.75
D	1.02	1.37	0.98	1.34	1.41

Such novel methodology origins by recognizing that the mass flow rate basically acts as a weighting function of the torque when computing the N_S, despite the formulation of choice (AVL/Ricardo). Since stationary testing evaluates the mass flow rate in conditions that are not realistic, this can be evaluated with other means capable of greater accuracy (e.g. 1D simulations). The procedure considers then the correlation between mass flow rate and torque obtained for stationary tests to hold also for dynamic conditions. The torque value for each lift (i.e. for each CA) can be therefore evaluated using the dynamic mass flow rate in conjunction with (5) or (6). The final step would be the integral averaging of these quantities over the whole intake stroke in order to calculate the R_S:

$$\omega_S(h) = \frac{L(h)}{I(h)} \rightarrow \omega_S(\theta) = \frac{L(\theta)}{I(\theta)} = \frac{\int_{\theta_{IVO}}^{\theta} M(\theta)\frac{d\theta}{\omega_m}}{I(\theta)} = \frac{\int_{\theta_{IVO}}^{\theta} K(\theta) N_{SR}(h(\theta))\dot{m}(\theta)\frac{d\theta}{\omega_m}}{I(\theta)} \tag{15}$$

$$R_S = \frac{1}{(\theta_{IVO} - \theta_{IVC})\omega_m}\int_{\theta_{IVO}}^{\theta_{IVC}} \omega_S(\theta)\, d\theta \tag{16}$$

where $K(\theta)$ is a quantity dependent on the N_S formulation of choice (i.e. through (5) or (6)) and $I(\theta)$ is the moment of inertia of the fluid present in the cylinder at CA θ. The novel methodology here proposed is subject of current work and will be more extensively described in an upcoming paper.

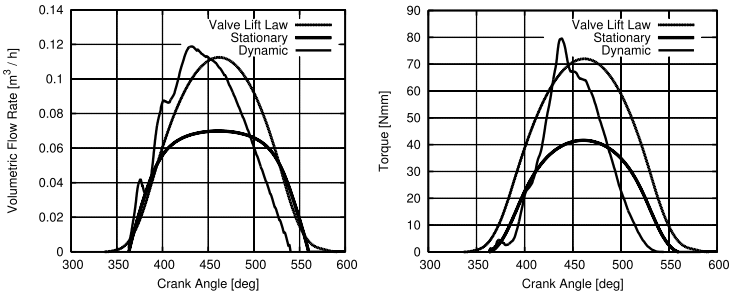

Fig. 12: Left: Dynamic and stationary mass flow rates for engine C. Right: Dynamic and stationary torque for engine C. To be noted that for the Valve Lift Law only the profile shape has been reported.

5. Conclusions

In the present work a numerical methodology aimed at developing a virtual engine head test bench has been proposed. The methodology has been assessed and a comparison between numerical simulation and experiments has been carried out. The results proved the viability of virtual testing as an interesting alternative to experiments. However, great care has to be taken when comparing prototypes having no geometrical similarity since, in this case, numerical simulation presented some limitations in the accuracy of predictions and in the possibility of making comparisons. The motivations for such behavior need to be further investigated and will be the subject of future work. Furthermore steady state testing allowed to evaluate the capabilities of two different formulations available to calculate the Swirl Ratio, namely Ricardo and AVL. The results demonstrated a substantial equal capability in approximating the experimental results and therefore both methods are eligible for virtual test bench applications. Finally, dynamic testing has shown some difficulties in establishing a clear link between steady flow bench and dynamic Swirl Ratios which could be overcame by employing the novel methodology here proposed based on 1D mass flow rate and steady testing torque data. More details on the procedure will be available in an upcoming paper.

Acknowledgement

The authors wish to thank Daniele Tassinari of University of Bologna for his precious contribution to the present work and for the many useful discussions.

References

[1] Commission, E.. Regulation (ec) no 715/2007 of the european parliament and of the council on type approval of motor vehicles with respect to emissions from light passenger and commercial vehicles (euro 5 and euro 6) and on access to vehicle repair and maintenance information. 2007.
[2] Heywood, J.B.. Internal Combustion Engine Fundamentals. Mcgraw-Hill; 1989.
[3] Ferrari, G.. Motori a combustione interna. Il capitello; 2001.
[4] Forte C., Bianchi G., Corti E.. Multicycle simulation of the mixture formation process of a pfi gasoline engine. SAE Technical Papers 2012;doi:10.4271/2011-01-2463.
[5] Costa M., Bianchi G., Forte C., Cazzoli G.. A numerical methodology for the multi-objective optimization of the di diesel engine combustion. vol. 45. 2014, p. 711–720. doi:10.1016/j.egypro.2014.01.076.
[6] Bianchi G., Cazzoli G., Forte C., Costa M., Oliva M.. Development of a emission compliant, high efficiency, two-valve di diesel engine for off-road application. vol. 45. 2014, p. 1007–1016. doi:10.1016/j.egypro.2014.01.106.
[7] Cazzoli G., Forte C., Vitali C., Pelloni P., Bianchi G.. Modeling of wall film formed by impinging spray using a fully explicit integration method. 2005, p. 271–280. doi:10.1115/ICES2005-1063.
[8] Challen B.. Diesel Engine Reference Book. 2nd ed.; Butterworth-Heinemann; 1999.
[9] Falfari S., Bianchi G., Nuti L.. 3d cfd analysis of the influence of some geometrical engine parameters on small pfi engine performances - the effects on tumble motion and mean turbulent intensity distribution. SAE Technical Papers 2012a;4. doi:10.4271/2012-32-0096.
[10] Falfari S., Bianchi G., Nuti L.. Numerical comparative analysis of in-cylinder tumble flow structures in small pfi engines equipped by heads having different shapes and squish areas. 2012b, p. 715–725. doi:10.1115/ICES2012-81095.
[11] Xu H.. Some critical technical issues on the steady flow testing of cylinder heads. SAE Technical Paper 2001;doi:10.4271/2001-01-1308.
[12] Trigui N., Choi W.. Characterization of intake-generated flow fields in i.c. engines using 3-d particle tracking velocimetry. SAE Technical Paper 1994;(940279). doi:10.4271/940279.
[13] Khalighi B.. Intake-generated swirl and tumble motions in a 4-valve engine with various intake configurations-flow visualization and particle tracking velocimetry. SAE Technical Paper 1990;(900059). doi:10.4271/900059.
[14] Brehm C., Whitelaw J., Sassi L., Vafidis C.. Air and fuel characteristics in the intake port of a si engine. SAE Technical Paper 1999;(1999-01-1491). doi:10.4271/1999-01-1491.
[15] Tassinari D.. Analisi critica delle metodologie numeriche e sperimentali per la valutazione del moto di swirl nei motori diesel. Master's thesis; UNIVERSITA' DI BOLOGNA; 2013.
[16] Ricardo. Steady state flowbench port performance measurement and analysis techniques. Tech. Rep. DP93/0704; Ricardo; 1993.
[17] AVL. Port development - flow test bench. Report collection; AVL List GmbH; 1995.
[18] AVL. AVL FIRE 2010 User Manual; 2010.